Neurobiology of Disease 124 (2019) 469–478

Contents lists available at ScienceDirect

Neurobiology of Disease

journal homepage: www.elsevier.com/locate/ynbdi

Mutant SOD1 prevents normal functional recovery through enhanced glial activation and loss of motor neuron innervation after peripheral nerve injury

Sarah Schram[a], Donald Chuang[b], Greg Schmidt[b], Hristo Piponov[b], Cory Helder[b], James Kerns[b], Mark Gonzalez[b], Fei Song[a,*], Jeffrey A. Loeb[a,*]

[a] Department of Neurology and Rehabilitation, Graduate Program in Neuroscience, University of Illinois at Chicago, 912 S. Wood Street, Chicago, IL 60612, USA
[b] Department of Orthopedics, University of Illinois at Chicago, 835 S. Wolcott Street, Chicago, IL 60612, USA

ABSTRACT

Background: Amyotrophic lateral sclerosis (ALS) is poorly understood with no effective therapeutics. One long entertained observation is that ALS may be precipitated focally by nerve injury. Many patients with ALS are athletes or veterans, and some have suffered nerve injuries at the site where ALS first presents. Here we explore how a genetic SOD1 mutation alters the inflammatory response and affects functional recovery after an environmental insult in a rat model.

Methods: Unilateral sciatic nerve crush injuries were performed in SOD1 G93A rats prior to disease symptom onset. Functional recovery was compared between injured wild-type littermates and uninjured SOD1 rats. Spinal cord tissues were analyzed quantitatively for SOD1 expression, glial reactivity, and motor neuron synaptic integrity.

Results: Injured SOD1 rats failed to recover and showed hastened functional decline with decreased survival. Injury induced extracellular SOD1 expression was associated with heightened, prolonged microglial and astrogial activation in the ventral horn. This inflammatory response spread to uninjured motor neuron pools and was associated with increased motor neuron synaptic loss.

Discussion: This study identified a relationship between genetic and environmental contributions to disease onset and progression in ALS. The findings suggest that injury induced SOD1 mutant protein induces a heightened and prolonged inflammatory response resulting in motor neuron degeneration through synaptic loss. Once initiated, this process spreads to adjacent motor neurons leading to contiguous spread of the disease. Treatments that suppress this heightened glial response could slow disease progression in ALS patients with focal sites of disease onset.

Significance statement: The contribution of environmental factors such as peripheral nerve insults in ALS is not well understood. Here we examined the effect of a single sciatic nerve injury in SOD1 (G93A) rats to explore the contribution of this environmental insult on disease onset and progression. After the injury, SOD1 animals failed to recover and had a more rapid functional decline. Histopathologically, SOD1 animals had heightened SOD1 expression, microglial and astroglial responses, and a reduction of motor neuron innervation. Taken together, these results provide a plausible mechanism of how the SOD1 mutated protein promotes an abnormal response to injury that leads to neurodegenerative changes in an ALS model that is amenable to therapeutic testing.

1. Introduction

Amyotrophic lateral sclerosis (ALS) is a neurodegenerative disease characterized by spreading paralysis due to motor neuron death. The disease progresses rapidly with average patient survival ranging from 2 to 5 years from diagnosis. Over 90% of ALS cases are sporadic, with no heritable genetic mutations. With variations in both the location of the onset of motor symptoms and the rate of disease progression, the heterogeneity makes understanding ALS pathology, clinical trials, and animal models particularly challenging. The degree of upper and lower motor neuron involvement also varies, with some patients presenting initially with upper motor neuron symptoms and others only developing them later as their disease progresses (Swinnen and Robberecht, 2014). In patients with lower motor neuron symptoms, a unifying characteristic of ALS is that regardless of disease onset location, neurodegeneration spreads contiguously along the spinal cord leading to progressive functional motor decline (Ravits and La Spada, 2009).

Why the disease starts in one specific group of motor neurons versus another is unclear. This clinical variance suggests that there are likely significant environmental factors contributing to where the disease starts. One long entertained hypothesis is that nerve or head trauma is an important environmental factor, as many patients with ALS have a history of these types of injuries (Valdes and Garbuzova-Davis, 2013; Horner et al., 2003; Miranda et al., 2008; Haley, 2003; Riggs, 1985, 1993, 1995, 2001; Piazza et al., 2004). A meta-analysis suggested that repeated head trauma, and timing of the injury increased the risk of

* Corresponding authors at: University of Illinois at Chicago, Department of Neurology and Rehabilitation, NPI North Bldg., Room 657, M/C 796, 912 S. Wood Street, Chicago, IL 60612, USA.
E-mail addresses: feisong@uic.edu (F. Song), jaloeb@uic.edu (J.A. Loeb).

https://doi.org/10.1016/j.nbd.2018.12.020
Received 22 August 2018; Received in revised form 11 December 2018; Accepted 26 December 2018
Available online 27 December 2018
0969-9961/

developing ALS (Chen et al., 2007). The increased prevalence of ALS in veterans and professional athletes, two populations that are more likely to have suffered nerve or brain trauma, further indicate a possible role of injury in disease onset (Lehman et al., 2012; Horner et al., 2003). Recent class I evidence further supports a positive association between ALS and physical activity, either at leisure time or with occupational activities (Visser et al., 2018).

Consistent with this human data, animal studies have demonstrated that nerve injury can modify the disease phenotype. Sharp et al. demonstrated that in the SOD1 mouse, a sciatic nerve crush induced premature changes in fatigue-resistance characteristics and muscle fiber type in the extensor digitorum longus and increased motor neuron loss in the ventral horn (Sharp et al., 2005). Facial nerve axotomy in an SOD1 mouse also showed increased motor neuron loss (Mariotti et al., 2002). In contrast, other studies have shown that a tibial nerve crush injury at the L5 nerve root or distal sciatic nerve led increased motor neuron survival in a subset of motor neurons once the disease initiated (Franz et al., 2009; Kong and Xu, 1999).

Exactly how peripheral nerve injury contributes to disease phenotype is not clear. One possibility is that peripheral nerve injury induces a strong central neuroinflammatory response by microglia and/or macrophages. Peripheral nerve injury has been studied extensively in models of chronic pain where it induces a strong microglial response in the dorsal horn of the spinal cord that has been shown to be mediated by soluble factors such as neuregulin that are released by the injured neurons (Calvo et al., 2010; David et al., 2015). Once activated, microglia adopt different phenotypes inducing either a pro-inflammatory/apoptotic or an anti-inflammatory/neuroprotective one (Kigerl et al., 2009). Activated microglia have also been implicated in synaptic modulation/elimination in developmental, post-injury, and neurodegeneration models (Alexander et al., 2008). Blocking this inflammatory microglial response in pain models has been shown to significantly reduce the development of chronic pain (Calvo et al., 2010, 2012).

Here, we performed longitudinal studies to determine the effect of mutant SOD1 overexpression on the functional recovery, disease progression, and ventral horn histopathology after a single sciatic nerve crush injury in the rat. We found that mutant SOD1 overexpression prevents animals from fully recovering, leads to more rapid disease progression, and produces a heightened inflammatory response associated with a loss of motor neuron innervation that could underlie functional deficits.

2. Materials and methods

2.1. Animals

Heterozygous SOD1(G93A) expressing and homozygous wild-type littermate rats (total $n = 53$; Taconic Biosciences Stock No 2148; Germantown NY 12526) were bred in house. Both males and females were used and balanced equally between groups. Genotyping was done according to Taconic Bioscience protocol with primers from IDT (forward primer: GTGGCATCAGCCCTAATCCA; reverse primer: CACCAGT GTGCGGCCAATGA). Animals were euthanized at specified time points for tissue collection (Fig. 1A). Mutant SOD1 expressing rats were considered end-stage when no longer able to right themselves or a > 20% loss of body weight occurred. Animals were given a lethal dose of ketamine HCL (135 mg/kg) and xyalzine (15 mg/kg) via intraperitoneal injection and underwent cardiac perfusion with saline and 4% paraformaldehyde (PFA) in PBS (Thermo-Fisher). Spinal cord and other tissue was collected for histological analysis. All experiments and animal use was approved by University of Illinois at Chicago Institutional Animal Care and Use Committee (IACUC).

2.2. Sciatic nerve injury and recovery

Sciatic nerve injury was modified from previously published injury protocols (Swett et al., 1991; Kerns, et al., 1991). Briefly, 10 week old rats were anesthetized with intraperitoneal injections of ketamine HCL (90 mg/kg) and xylazine (10 mg/kg). An incision was made in the left mid-thigh near the knee, allowing for splitting of the biceps femoris muscle. The sciatic nerve was exposed and all three branches (tibial, peroneal, and sural) were crushed individually just distal to the trifurcation. The crush consisted of a 30 s pinch using a forceps with bead stop to standardize force between injuries. Crush was verified by a break in the axoplasm, but an intact nerve sheath (Fig. 1B). The lesion site was blotted to assure hemostasis and kept moist with sterile 0.9% sodium chloride irrigation. Finally, the wound was closed in layers using continuous 6–0 bioresorbable sutures to re-approximate the muscle and interrupted mattress 4–0 ethilon sutures for the skin. Animals were given a subcutaneous injection of buprenorphine SR for acute pain management post-operatively.

Functional recovery was assessed using the Extensor Postural Thrust (EPT) test as previously described (Koka and Hadlock, 2001; Hulata et al., 2008). Animals were suspended above a scale with a single limb lowered to contact the scale surface, allowing force generation against the plate. Five measures per leg were recorded and averaged. Prior to surgery, animals were handled a minimum of 5 times and exposed to the EPT test procedure to reduce anxiety. A pre-surgical baseline was recorded at 9 weeks of age, 1 week prior to surgery. Functional strength was normalized to the pre-surgical baseline. Experimenters were blinded to animal genotypes throughout the study to prevent bias.

2.3. Immunohistochemistry

Following euthanasia, tissue was harvested and fixed overnight in 4% PFA, followed by another 24 h in 30% sucrose. Tissues were then embedded and frozen in OCT (Tissue-Tek®, Sakura Finetek). Tissues were sectioned at 12 µm thickness using a Leica CM1850 cryostat. Microglia were stained using a polyclonal rabbit anti-Iba1 (1:500; Wako, 019–19741) and a secondary goat anti-rabbit alexafluor488 conjugate (1:250; Abcam, ab150077). Astrocytes were stained with polyclonal rabbit anti GFAP (1:200; Dako, Z0334) and a secondary goat anti-rabbit alexafluor647 conjugate (1:250; Abcam, ab150079). Synapses were stained with rabbit anti-synaptophysin (1:500, Dako, A0010) and and a secondary goat anti-rabbit alexafluor488 conjugate (1:250; Abcam, ab150077). Motor neurons were stained with a fluorophore conjugated Nissl stain (1:300, NeuroTrace Red; Thermo Fisher, N21482). SOD1 was stained with rabbit anti-SOD1 (1:200; Abcam ab16831) and a secondary goat anti-rabbit alexafluor488 conjugate (1:250; Abcam, ab150077). All primary antibodies were incubated over night at 4° C and all secondary antibodies were incubated for 1 h at room temperature. Slides were imaged using a Leica ctr5500 scope, LS200US laser box, Qimaging exi aqua camera, and Surveyor imaging software and confocal images were taken using a Zeiss Laser Scanning Microscope (LSM) 510 Meta and ZEN Imaging Software.

2.4. Glial activation analysis

Glial activation was calculated using MetaMorph® Image Analysis software. Briefly, colour channels were separated and a threshold was set to determine positively stained structures versus background stain. Regions of a standard size and shape were used to encompass anatomical regions containing Nissl-positive cells (dorsal horn, lateral motor column, and medial motor column; Fig. 1C). Once regions of interest were set, a percentage of the standard region area with positive stain was calculated using the region measurements feature. As activated glia have larger cell bodies and changes in morphology, greater activation was indicated by a greater percentage of area with positive stain. An average of 3 slides from the L4-L5 spinal cord region per animal was calculated and investigators were blinded to experimental conditions.

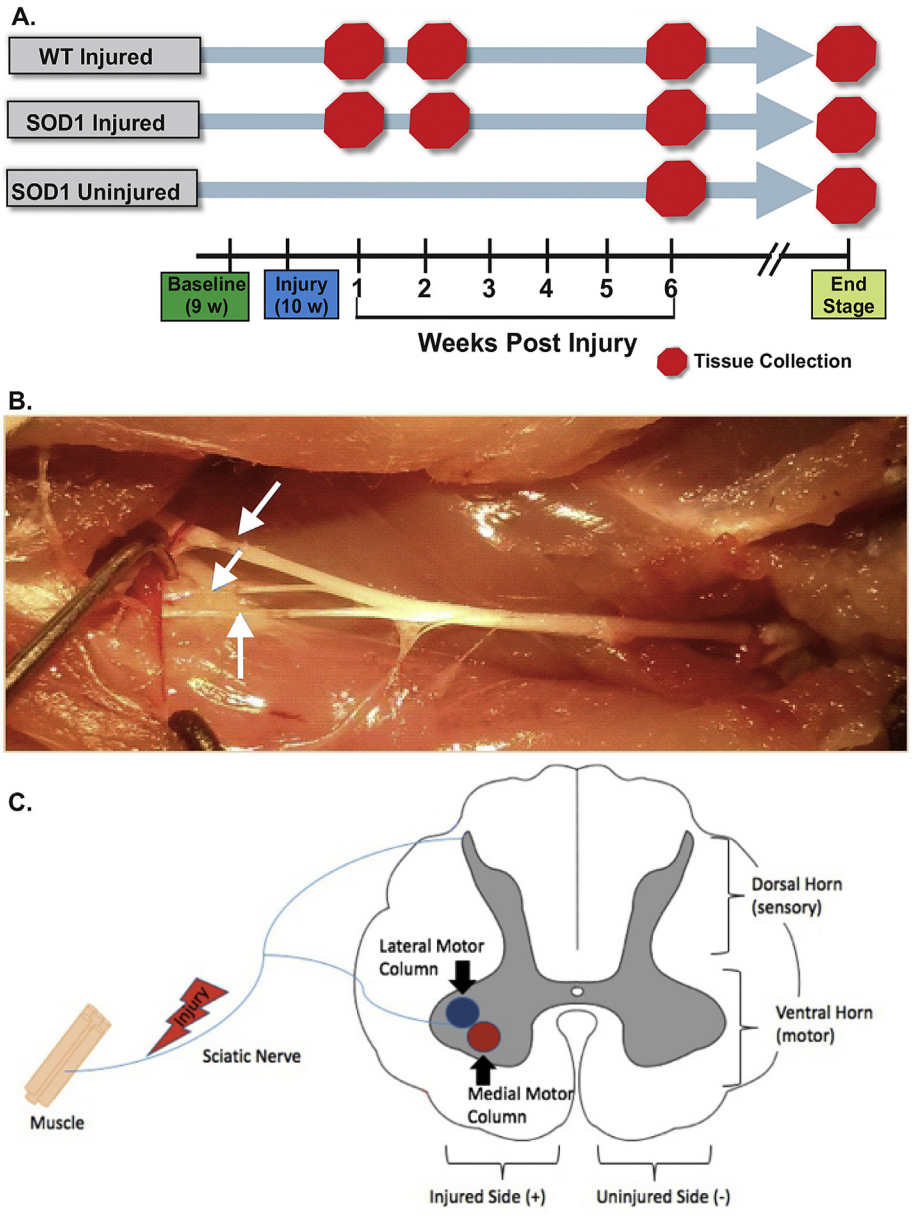

Fig. 1. Experimental design for determining the effect of nerve injury on function and neuropathology in SOD1 rats.
A. Pre-surgical baseline strength was assessed at 9 weeks of age and a single, unilateral nerve crush injury was performed at 10 weeks in SOD1 and wild-type (WT) rats. Animals were euthanized at 1, 2, and 6 weeks post-injury and at end-stage. Uninjured SOD1 control animals were euthanized at 16 weeks of age (prior to motor symptoms) or end-stage. Collection time points are indicated by the red shapes. **B.** The sciatic nerve was exposed mid-thigh. Each branch of the nerve was crushed just distal to the trifurcation and verified by a break in the axoplasm (white arrows). **C.** This is a schematic showing regions selected for histological analysis. The lateral motor column contains cell bodies of motor neurons directly affected by crush while the adjacent medial motor column contains uninjured motor neurons as a means to examine disease spread.

2.5. Synaptic density analysis

Synaptic density was calculated using MetaMorph® Image Analysis software. Cross sections of motor neurons were identified by positive Nissl stain, size, and morphology. In order to remain consistent, only cross-sections of neurons were quantified. A threshold of positive synaptophysin stain above background was determined and the cell membrane was traced to encompass synapses on the perimeter of the cell (Fig. 5B). The percent of the region positive for synapse stain was determined using the region measurements feature. Three to four neuronal cross sections per animal in the L4-L5 region of the spinal cord were quantified and investigators were blinded to experimental conditions.

2.6. SOD1 expression analysis

SOD1 aggregation was calculated using MetaMorph® Image Analysis software. Colour channels were separated and a threshold was set to determine positively stained structures versus background stain. Regions of a standard size and shape were used to encompass anatomical regions in the ventral horn. Once regions of interest were set, the Integrated morphometry analysis feature was used to determine the total area of SOD1 positive stain.

2.7. Experimental design and statistical analysis

All nerve injuries were given at 10-weeks of age, and animals were assigned to various tissue collection time points (Fig. 1A). Functional recovery was tracked weekly using the EPT test as described above. Multiple *t*-test comparisons were done by week, using the Holm-Sidak method for multiple comparisons. To compare functional loss over time, an ordinary one-way ANOVA was calculated using Bartlett's test and survival curves were determined using the Mantel-Cox test. Histological analysis was made using student's t-test to compare regions. All statistical analysis was done using GraphPad Prism software.

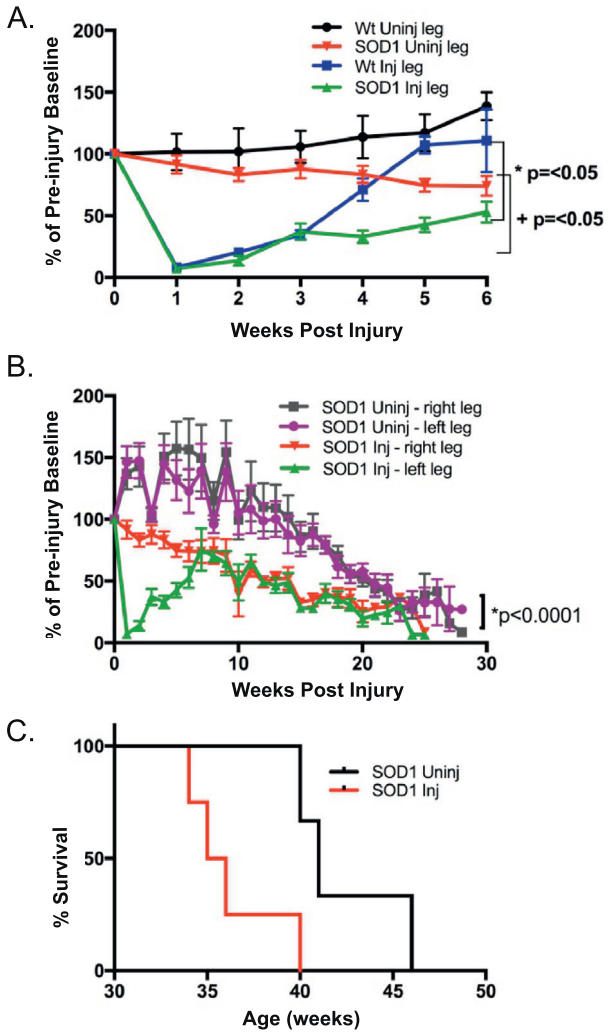

Fig. 2. Injured SOD1 rats fail to recover and show more a rapid functional decline compared to age-matched uninjured SOD1 rats.
A. Functional recovery between WT (n = 11) and SOD1 (n = 10) animals was tracked using extensor postural thrust (EPT) testing and normalized to the pre-surgical baseline for each animal. At 5 weeks, the WT injured limb had recovered to the pre-surgical baseline while the SOD1 injured limb showed significant functional impairments: $t(19) = 23.21$, $p = 1.3 \times 10^{-14}$, 5 week WT uninj vs SOD1 uninj: $t(19) = 19.74$, $p = 2.4 \times 10^{-13}$, t-test with Holm-Sidak method used to correct for multiple comparisons, alpha = 0.05; ANOVA ($F(3, 18) = 11.13$, $p = .002$. **B.** Functional strength of limbs was compared between injured (n = 10) and uninjured (n = 8) SOD1 rats with the EPT test and normalized to week 9 baseline. Injured SOD1 rats showed a more rapid functional decline compared to uninjured SOD1 rats ($F(3, 106) = 12.44$, $p < .0001$, ANOVA. **C.** SOD1 rats receiving the injury reached end stage sooner (n = 4, mean 36.25 weeks, SD = 2.63) than direct littermates that were not injured (n = 3, mean 42.33 weeks, SD = 3.22), however due to low animal numbers for a given litter, this result did not reach significance using the Mantel-Cox test of survival, $p = .126$.

3. Results

3.1. SOD1 rats fail to recover after a single peripheral nerve crush injury

SOD1(G93A) rats (SOD1, n = 10) and wild type littermates (WT, n = 11) were assessed for baseline functional strength at 9 weeks of age using the extensor postural thrust (EPT) test, which independently measures motor strength for each hind limb (Fig. 1A). This time point was chosen because it is well before any expected motor symptoms in SOD1 rats. At 10 weeks of age, the sciatic nerve was exposed and a single crush was applied distal to the trifurcation in all three branches and verified by visualizing a break in axoplasm (seen as a gray translucent nerve), but leaving the nerve sheath intact (Fig. 1B, arrows). EPT was measured weekly and animals from each group were euthanized for tissue collection at 1, 2, and 6 weeks post-injury and at end stage disease (Fig. 1A). At each of these time points, both the lateral motor column containing the injured motor neurons and the adjacent, uninjured medial motor column were examined histologically (Fig. 1C).

Following nerve injury, recovery was assessed weekly by a blinded investigator using EPT and recorded as a percentage of pre-surgery baseline (Fig. 2A). While WT animals fully recovered their injured leg function by 5 weeks post-injury, SOD1 animals showed some improvement, but never returned to their baseline levels (5 week WT inj vs SOD1 inj: $t(19) = 23.21$, $p = 1.3 \times 10^{-14}$, t-test with Holm-Sidak method used to correct for multiple comparisons, alpha = 0.05). Surprisingly, the uninjured leg of SOD1 animals also were functionally impaired compared to the uninjured leg in WT animals (5 week WT uninj vs SOD1 uninj: $t(19) = 19.74$, $p = 2.4 \times 10^{-13}$, t-test with Holm-Sidak method used to correct for multiple comparisons, alpha = 0.05). These results not only show that mutant SOD1 prevents normal limb recovery following nerve injury, but also promotes a functional decline on the opposite, uninjured side ($F(3, 18) = 11.13$, $p = .002$, ANOVA).

3.2. Motor function declines more quickly in injured SOD1 rats than uninjured SOD1 rats

In order determine the effect of nerve injury on disease progression, we compared serial measures of hind limb strength in injured and uninjured SOD1 rats. Functional ability was tracked weekly using EPT and normalized to pre-surgical or 9 week old (age-matched) baseline in injured SOD1 animals (n = 10) and uninjured SOD1 animals (n = 8). Following injury, the strength in both injured and uninjured legs decreased earlier and more rapidly than was seen in the uninjured SOD1 animals ($F(3, 106) = 12.44$, $p < .0001$, ANOVA). Uninjured SOD1 animals had normal (defined as 100% or greater than baseline) functional strength until 25 weeks of age (corresponding to 15 weeks post injury), versus only 11 weeks of age (corresponding to 1 week post injury) in the injured group (uninjured leg) (Fig. 2B). Because of the high degree of variability in survival reported from litter to litter in the SOD1 rat, we only compared survival between SOD1-expressing direct littermates that were either injured (n = 4) or uninjured (n = 3). While injured animals within the same litter showed decreased survival (mean 36.25 weeks, SD = 2.63) compared to uninjured littermates (mean 42.33 weeks, SD = 3.22), the small group size likely prevented reaching statistical significance (Mantel-Cox test of survival, $p = .126$) (Fig. 2C). Taken together, these results show that a single peripheral nerve injury causes not only a failure to recover, but also precipitates a more rapid decline in function with mutant SOD1 expression.

3.3. Injured SOD1 animals have heightened and prolonged microgliosis and earlier than expected astrogliosis

The mechanism by which the mutant SOD1 expression leads to failed recovery and more rapid disease progression after axonal injury is not clear, but could relate to altered signaling and cellular responses from the injured motor neurons. Peripheral nerve injury leads to axonal degeneration of both motor and sensory neurons. Activation of microglia is well known to occur in the dorsal horn of the spinal cord in models of chronic pain following peripheral nerve injury, but this is less well studied in the ventral horn (Calvo et al., 2010; Kerns and Hinsman, 1973). In the first week following injury, both WT (n = 6) and SOD1 (n = 5) animals show elevated microgliosis using Iba1 staining (green) on the injured side of the spinal cord in the dorsal horn, lateral motor column, and medial motor column, shown (Fig. 3). While there was no significant difference in this inflammatory response in the dorsal horn of the spinal cord (Fig. 3B and E), there was a significantly elevated and

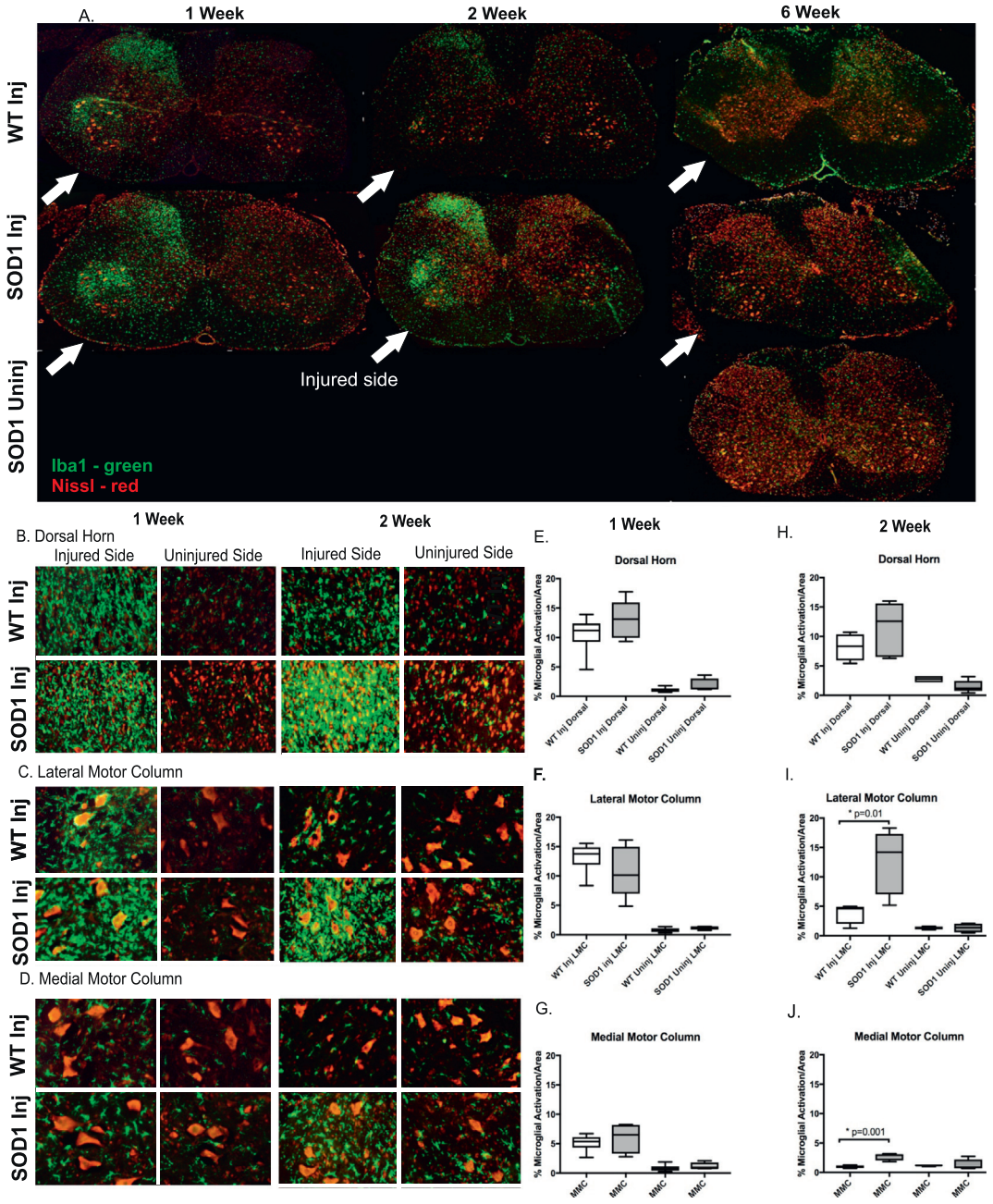

Fig. 3. Injured SOD1 animals show abnormally elevated and prolonged microgliosis in the ventral horn compared to WT controls.
A. Cross sections at L4-L5 showed marked microglial activation on the injured side (white arrows) of the spinal cord following injury (Iba1, green). Many of these microglia were seen to fully engulf injured motor neurons (Nissl, red) in the SOD1 animals. **B-D**. Magnified views are shown of the dorsal horn, lateral and medial motor columns, respectively, at 1 and 2 weeks post-injury from injured WT (1 week, $n = 6$; 2 week, $n = 4$) and injured SOD1 animals (1 week, $n = 5$; 2 week, $n = 5$). **E-J**. Quantification of microglial activation in each of these regions was obtained in a blinded manner using 3 sections per animal. A significant increase in microgliosis was seen at 2 weeks post injury on the injured side of the lateral ($t(7) = 3.056$, $p = .0184$, unpaired t-test) and medial ($t(7) = 5.336$, $p = .001$) motor columns. (For interpretation of the references to colour in this figure legend, the reader is referred to the web version of this article.)

prolonged response in the ventral horn of SOD1 animals (Figs. 3C-G). By the second week after injury, the microglial activation in WT animals ($n = 4$) had subsided while the, injured SOD1 animals ($n = 5$) showed sustained microglial activation. Higher power views show activated microglia completely engulfing motor neuron cell bodies (Nissl stain, red). By 6 weeks post injury the microglial activation subsided and was comparable to uninjured SOD1 age-matched controls (WT inj $n = 4$, SOD1 inj $n = 4$, SOD1 uninj $n = 5$) (Fig. 3A-D). Quantitative analysis of this microglial response in the dorsal horn, the lateral motor column (containing cell bodies of crushed motor neurons), and the medial motor column (adjacent in spinal cord but unaffected by the crush) were performed using the contralateral side as an internal control for each section. Microglial activation in SOD1 animals was significantly elevated in the lateral motor column of the injured side at 2 weeks compared to controls ($t(7) = 3.06$, $p = .02$, unpaired t-test). The medial motor column region also showed increased in sustained microgliosis at 2 weeks ($t(7) = 5.34$, $p = .001$; Fig. 3J).

In addition to microgliosis, astrogliosis occurs in the spinal cord of symptomatic SOD1 animals (Howland et al., 2002). Both microgliosis and astrogliosis are present in human ALS spinal cord (Song et al., 2014, 2014). Astroglial levels in injured SOD1 animals ($n = 4$) were not appreciably different from age-matched injured WT animals ($n = 5$)

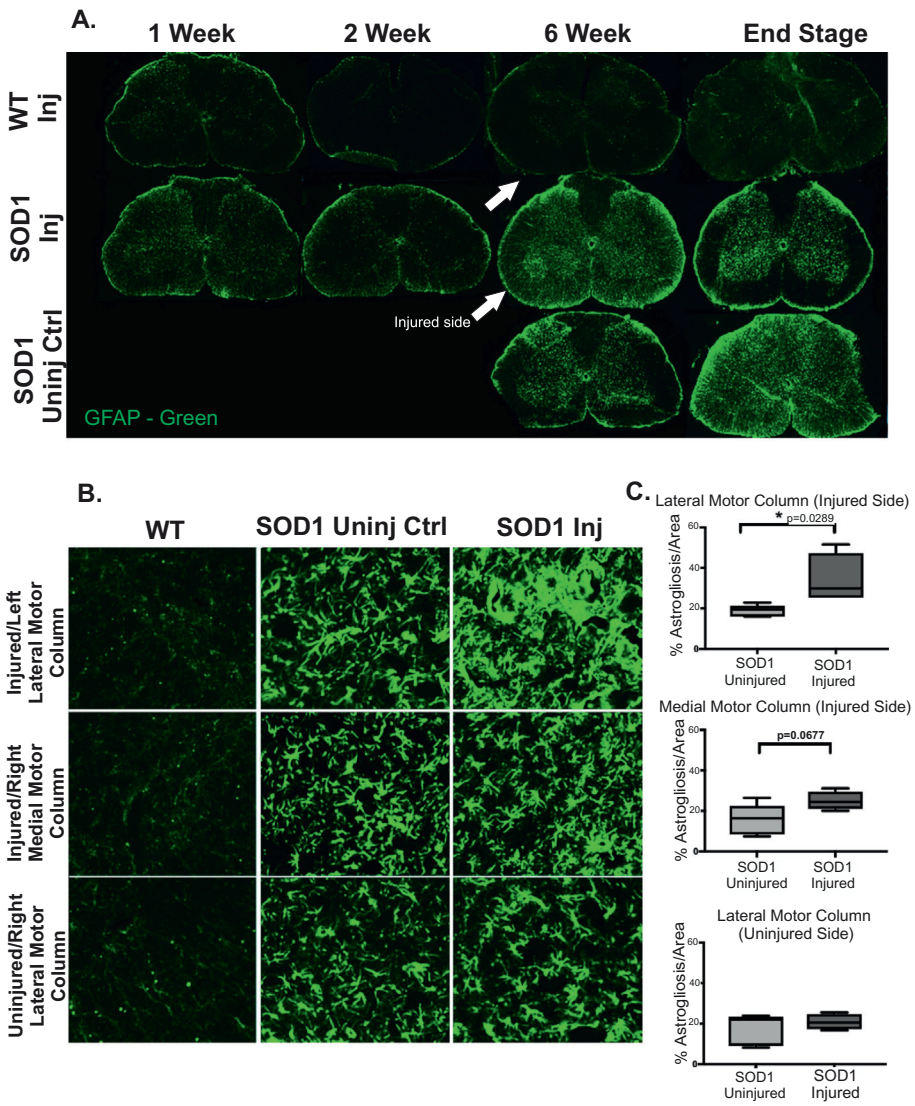

Fig. 4. Injury induces delayed, but focal astrogliosis in SOD1 animals.
A. Cross-sections at L4-L5 comparing the degree of astrogliosis following injury in WT, injured SOD1, and uninjured age-matched SOD1 animals (GFAP, green) show markedly more astrogliosis in the injured SOD1 spinal cord at 6-weeks post-injury (16 weeks of age). **B**. Magnified images of the lateral motor column show focally increased astrogliosis in injured SOD1 animals. **C-E**. Quantitative measurement of astrogliosis between uninjured ($n = 5$) and injured ($n = 4$) SOD1 rats shows a significant increase in GFAP stained astrocytes of the lateral motor column on the injured side ($t(7) = 2.74$, $p = .029$, unpaired t-test). This also appears to spread to adjacent, uninjured motor neurons in the medial motor column ($t(7) = 2$, $p = .068$, unpaired t-test). (For interpretation of the references to colour in this figure legend, the reader is referred to the web version of this article.)

during the first 2 weeks after injury. However, by the sixth week post-injury, the SOD1 animals showed a markedly elevated astrocytic reactivity in the ventral horns containing injured motor neurons (lateral motor column). This astrocytosis was significantly higher than that of uninjured age-matched SOD1 animals, which also show increased levels of GFAP. This astrogliosis remains elevated and expands throughout the spinal cord by end stage, similar to was is seen in the uninjured SOD1 control group (Fig. 4A). Quantitative analysis of GFAP expression at this time showed a significant increase in reactive astrocytes in the lateral motor column of the injured side compared to uninjured SOD1 controls ($t(7) = 2.74$, $p = .03$, unpaired t-test) (Fig. 4B, C). While not highly significant, increased gliosis around uninjured medial motor neurons was also observed ($t(7) = 2$, $p = .068$, unpaired t-test) (Fig. 4B, D). Astrogliosis was greatest on the injured side, as there were no differences in the uninjured side for the lateral motor column ($t(7) = 0.807$, $p = .45$, unpaired t-test) (Fig. 4B, E).

Taken together, a single peripheral nerve injury in SOD1 rats results in a stronger and more prolonged microglial response followed by an earlier than expected astroglial response that appears to spread to nearby, uninjured motor neurons in the spinal cord.

3.4. Mechanism of nerve injury induced neurodegeneration by mutant SOD1

The observation that nerve injury leads to microglial activation in the spinal cord has been well-studied in models of chronic pain and injury (Luo et al., 2014; Calvo et al., 2012; Kerns and Hinsman, 1973). Exactly what causes the enhanced glial response observed here in SOD1 animals and how this leads to the observed decline in motor function is not clear. One possibility is that nerve injury induces mutant SOD1 expression that, in turn, promotes microglial activation. Increased secretion of extracellular, mutant SOD1 has been shown to promote a strong, toxic inflammatory response (Urushitani et al., 2005). Consistently, Fig. 5A and D show increased, extracellular SOD1 expression levels near injured motor neurons in the animals 2 weeks after injury ($n = 5$, $t(8) = 2.66$, $p = .03$).

In order to understand how an increased inflammatory response leads to neurodegeneration, we quantified motor neuron innervation density. We found a nearly 2-fold reduction of somatic synaptic structures in the injured SOD1 rats (Fig. 5B, C, and E). While there was no difference in the synaptic density between wild type ($n = 3$, 3–4 neurons/region/animal) and uninjured SOD1 animals ($n = 3$, 3–4 neurons/region/animal), there was a highly significant reduction in the injured SOD1 animals ($n = 4$, 3–4 neurons/region/animal ($F(2,28) = 22.36$, $p < .0001$) (Fig. 5E). This profound reduction in motor neuron cell

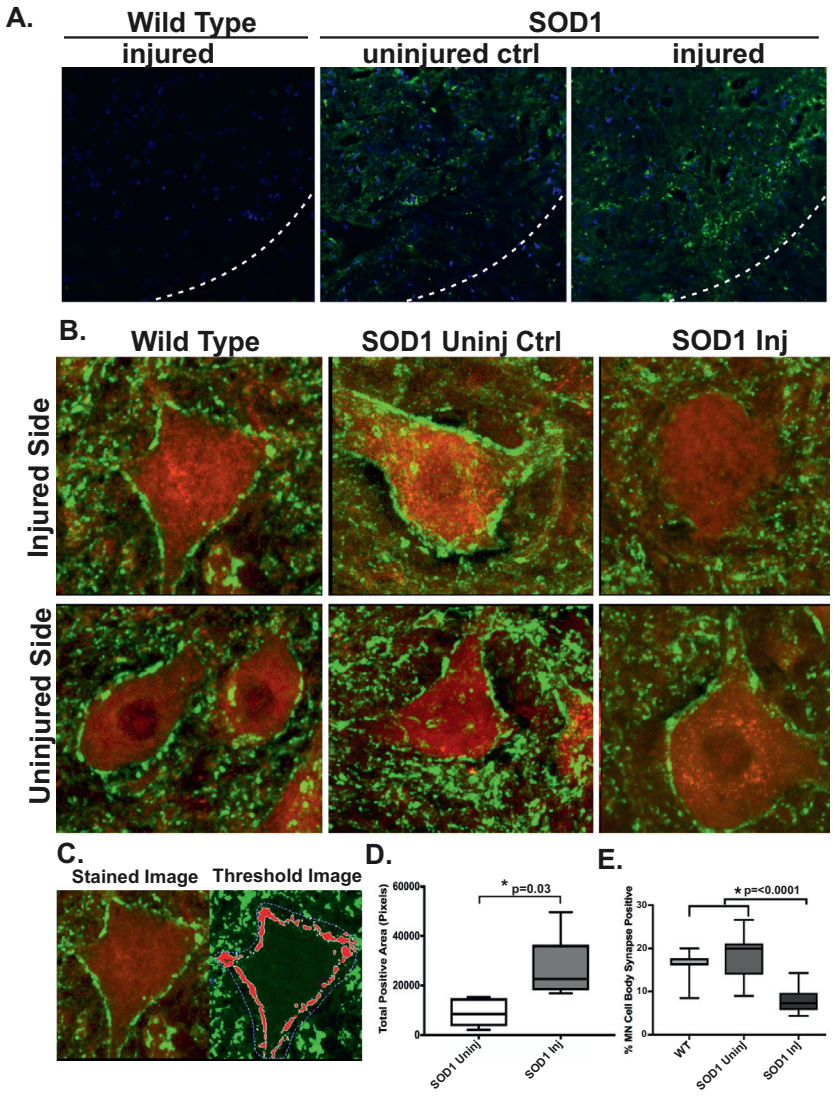

Fig. 5. Increased extracellular SOD1 surrounding injured motor neurons early could lead to a marked reduction in innervation.

A. SOD1 protein expression was increased in the extracellular space of the ventral horn on the injured side of the spinal cord at 2 weeks after injury. **B**. Synaptic density was significantly reduced in these same regions 6 weeks after injury. Synaptic density was quantified on individual motor neuron cell bodies using synaptophysin antibodies (green) on confocal images through the nucleus of motor neurons (Nissl stain, red). **C**. The percentage of the cell membrane on each motor neuron covered with synaptophysin stained synapses was determined using a custom script with Metamorph software. **D**. Quantitative measures of extracellular SOD1 in the ventral horn at 2 weeks following injury on injured and uninjured side of SOD1 animals show increased, extracellular protein aggregation on the injured side ($n = 5$, $t(8) = 2.66$, $p = .03$). **E.** Synaptic Density (% MN cell body cross-section perimeter positive for synaptophysin stain) was compared between WT ($n = 3$), uninjured SOD1 ($n = 3$) and injured SOD1 animals ($n = 4$) (3–4 neurons/region/animal). A significant decrease in synaptic density was seen in the lateral motor column of injured SOD1 animals ($F(2,28) = 22.36$, $p < .0001$). (For interpretation of the references to colour in this figure legend, the reader is referred to the web version of this article.)

body innervation was clearly related to the injury since the contralateral side of the injured SOD1 animals had a normal synaptic density.

4. Discussion

4.1. An animal model to understand the interplay between environmental and genetic contributions for ALS

Our results show that a single nerve crush injury, which causes only temporary impairment in wild type animals, leads to failure to recover and hastened functional decline in the SOD1 rat. This observation is consistent with a variety of clinical observations postulating that in genetically vulnerable patients, an injury that would normally not cause untoward effects is enough to initiate the disease (Valdes and Garbuzova-Davis, 2013; Yip and Malaspina, 2012). Intriguing anecdotal and case studies ALS patients suggest a relationship between nerve and brain injury and ALS (Valdes and Garbuzova-Davis, 2013; Horner et al., 2003; Miranda et al., 2008; Haley, 2003; Riggs, 1985, 1993, 1995, 2001; Piazza et al., 2004; Chen et al., 2007; Lehman et al., 2012, Visser et al., 2018). Some of these studies provide class I evidence, yet others may be limited by inconsistent methodologies and definitions of the nature and severity of trauma. Additionally, ALS is a heterogeneous disease and different patient subtypes may experience a variety of environmental triggers, making the epidemiology challenging. The severity and timeframe of injury could also play a role in symptom development and therefore be under-reported in certain medical histories.

Previous studies investigating the role of injury in the SOD1 animal model have shown variable results, some showing a more severe phenotype and others suggesting earlier injury can be protective (Franz et al., 2009; Kong and Xu, 1999; Sharp et al., 2005, 2018, & Mariotti et al., 2002). There are a number of differences between these studies including injury location, severity, and age at time of injury. These could lead to important variations in injury response, affecting recovery and survival. Furthermore, genetic drift within the rat model has led to differences in survival across litters (Taconic), making direct comparisons between studies difficult. For example, Franz et al., reported mean survival in their study to be 23 weeks, which was a much more severe phenotype than the colony used in this study which showed survival of uninjured controls closer to 35 weeks. This makes controlling for presymptomatic disease stages across studies challenging. To address this, studies conducted here included direct littermate controls to compare the effects of injury. While this approach resulted in smaller group sizes, this accounts for some variation between litters and strengthens the data presented here.

Unlike the SOD1(G93A) mouse model, the rat can have forelimb or bulbar onset, similar to what can be seen in patients with ALS

(Smittkamp et al., 2010). While quantitative assessment of limb strength was only conducted in the hindlimb, it is worth noting that due to the spreading nature of the pathology, a decreased time to end-stage suggests a global acceleration of symptoms which were initiated from the hindlimbs. Further studies that explore nerve injuries in the forelimb versus hindlimb, proximal versus distal nerve location, and single versus repeated injury could help to understand the relationship between nerve injury, the site of disease onset, and how this affects disease progression and survival. Results from these animal studies, in turn, could help shed light on how best to identify risk factors and prognosis in patients with ALS. Similar studies in other ALS animal models might be helpful to determine if the increased susceptibility to injury observed here in the SOD1 model plays a more general role in ALS disease progression with different underlying genetic abnormalities, such as C9orf72, TDP-43, FUS, or profilin (Philips and Rothstein, 2015).

4.2. Mutant SOD1 overexpression leads to a heightened and more prolonged inflammatory response

As a means to understand how SOD1 mutant protein prevents recovery after nerve injury and leads to a more rapid disease course, we examined the interactions between glia and motor neurons in the spinal cord. Fig. 6 qualitatively summarizes our sequential findings. Perhaps the most salient of these was a heightened and prolonged microglial inflammatory response. At this time point, microglia were seen engulfing injured neuronal cell bodies (Fig. 3). Compared to WT animals,

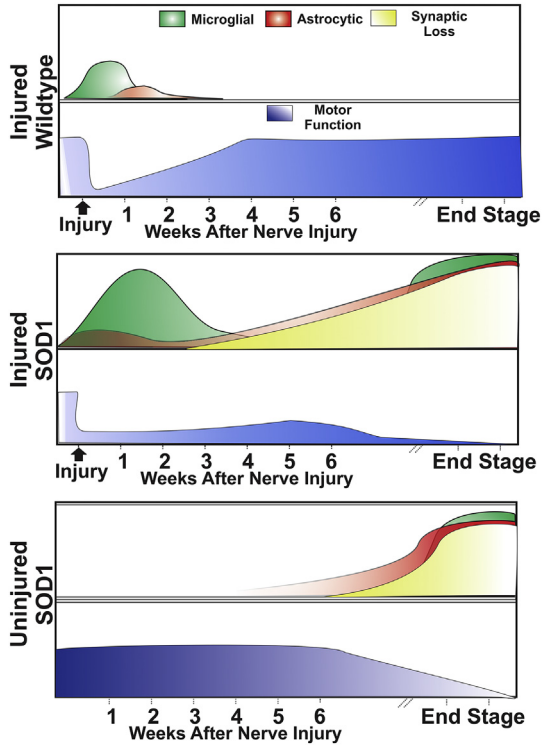

Fig. 6. Time course of injury-induced functional, inflammatory, and neuronal changes in the SOD1 rat.
This figure summarizes the longitudinal effects of mutant SOD1 protein both on motor function and cellular pathophysiology after a single sciatic nerve injury. While WT animals recovered fully from the injury within 5 weeks, they had only mild microgliosis/astrocytosis in the acute recovery stage. In contrast, injured SOD1 animals failed to recover and showed increased and sustained microgliosis followed by a premature astrocytic recruitment and neuronal synaptic loss. This model combines an environmental insult with a genetic defect can help elucidate the functional and physiological effects of ALS disease onset and progression that could be used to develop targeted therapeutics.

the expression of mutant SOD1 produced a stronger and more long-lasting activation of microglia surrounding injured motor neurons following nerve injury. Four weeks following the microglial response we observed focal and premature astrogliosis, well after the microglial response subsided. While we did not see significant neuronal loss at this stage, quantitative analysis of synaptic innervation of the injured motor neurons revealed a 2-fold reduction in innervation of motor neuron cell bodies. This synaptic loss was not seen in injured wildtype animals nor in age-matched uninjured SOD1 animals.

While the sequential glial activations observed here were most significant in the lateral motor column containing the injured motor neurons, inflammation was also seen to spread to the adjacent medial motor neuron column containing uninjured motor neurons. Previous anatomical studies have identified motor neuron pools innervating different muscles and as such would not have been affected by the crush (Davis-Dusenbery et al., 2014; Kanning et al., 2010). The anatomical proximity while innervating different muscles support our hypothesis of spreading in that it appears that glial reactivity is not isolated to areas directly affected by the crush, but is also seen in nearby motor neuron pools which would then also be affected by inflammatory activity despite having not been injured. This is consistent with previous research in rats showing microglial activation spread throughout the spinal cord, including the contralateral side (Kerns and Hinsman, 1973). In this way we propose a spreading mechanism linked to inflammation which may provide a plausible mechanism by which the ALS disease process spreads through the spinal cord and would be consistent with clinical observations in patients who have focal weakness that later spreads contiguously (Ravits and La Spada, 2009). While this study only examined the potential of local glial spread, future studies should examine other areas along the spinal cord for inflammatory activity and changes in cellular pathology.

Two weeks after the injury, increased levels of extracellular-appearing mutant human SOD1 protein was observed only on the injured side that also showed a markedly enhanced and more prolonged inflammatory response. Exactly what cell type this SOD1 protein is coming from is not clear, however, previous studies suggest that mutant SOD1 expressed in both microglia and astrocytes can promote disease progression (Yamanaka et al., 2008; Nagai et al., 2007). One possibility is that the mutant SOD1 protein reduces the ability of microglia to return to their normal resting state following the injury, resulting in a more prolonged recovery phase leading to toxic chain reaction between motor neurons and microglia that spreads to adjacent spinal cord regions. Such a toxic feedback loop could also originate from SOD1 mutant protein expression in motor neurons (Urushitani et al., 2005). Another possibility is that stress granules can form and play a role in neuronal cell death in ALS (Liu-Yesucevitz et al., 2010; Li et al., 2013). Stress granules are small inclusions of mRNA and RNA binding proteins formed in normal cells that can result from the stress of neuronal injury. Under normal conditions, stress granules are formed and cleared as the cellular stress resolves, however, in vivo models and post-mortem human tissue from ALS patients suggest a failure to clear stress granules, including those caused by injury (Anderson et al., 2018; Liu-Yesucevitz et al., 2010). While a direct association between mutant SOD1 and stress granules is not firmly established, stress granule induced toxicity is another possible mechanism that could lead to motor neuron degeneration (Kedersha et al., 2013).

One signaling system that known to mediate neuron-microglia interactions following peripheral nerve injury is the growth factor neuregulin (Calvo et al., 2010; Calvo et al., 2011). Secreted forms of neuregulin are released from transmembrane protein precursors through a regulated cleavage mechanism to activate their receptors on nearby glial cells (Esper and Loeb, 2004, 2009). We have recently shown that neuregulin receptors are constitutively activated on microglia in the SOD1 mouse model and in human spinal cord tissues, both in the ventral horn and the corticospinal tracts (Song et al., 2012, 2014). Blocking the effects of neuregulin could therefore be a potential

therapeutic target by preventing the further spread of microglial activation. In fact, studies in chronic pain following nerve injury show that blocking neuregulin signaling in the spinal cord following injury can prevent microglial activation as well as the downstream synaptic changes thought to lead to chronic pain (Calvo et al., 2012). For ALS, we have recently found that a novel fusion protein can slow disease progression and increase survival in the SOD1 mouse model (Liu et al., 2018).

In addition to microglial activation, we found a delayed, but prominent astrogliosis 6 weeks post-injury. It is possible that the microglia trigger this astroglial response or that the injured motor neurons stimulate astrogliosis directly. One possibility is the astroglial response is initiated through glutamatergic signaling and ongoing excitoxicity, which is thought to be a potential mechanism of ALS disease progression (Blasco et al., 2014). Astrocytes both respond to and produce cytokine signaling that could also contribute to propagating an inflammatory feedback loop and induction of neuronal damage (Liddelow et al., 2017).

4.3. Nerve injury leads to early synaptic stripping that could underlie motor neuron neurodegeneration

In order for this enhanced inflammatory response to promote disease onset and progression, it is critical to understand how it would lead to motor neuron degeneration. One possibility is the role of nitric oxide, which has been hypothesized to be involved in synaptic loss and may be increased in SOD1 mutant animals (Moreno-Lopez et al., 2011) Microglia-dependent synaptic stripping has also been implicated in a number of neurodegenerative diseases (Alexander et al., 2008). We found significant synaptic loss on injured motor neurons as a result of the SOD1 mutant expression (Fig. 5). Injured and nearby motor neurons in the SOD1 animals were often engulfed by microglia in the acute recovery phase. Loss of synaptic integrity and signaling can induce apoptosis in neurons (Alexander et al., 2008). Preventing the loss of these synapses either through blocking microglia or stabilizing these connections could also be a therapeutic strategy.

Despite these alterations in synaptic connectivity, no decrease in the number of motor neurons was observed. Motor neuron somal counts were conducted using Metamorph quantitation methods. No differences were seen between experimental groups, or when comparing the injured to uninjured side in the same animal (data not shown). It is possible that motor neuron loss follows synaptic dennervation and was outside the time window that we examined here. Future studies could incorporate later time points to better understand the sequence of neuronal loss following synaptic pruning. Similarly, while beyond the scope of the present study, there are likely to be similar synaptic changes following injury at the neuromuscular junction that could be instrumental in the degenerative process.

4.4. A new preclinical model for ALS

Many promising drug candidates that extend survival in SOD1 animals have failed to be beneficial in human clinical trials, including immunomodulatory therapies (Mitsumoto et al., 2014; Gordon et al., 2007; Drachman et al., 1994; Fournier et al., 2018). While some of these failures may have come from underpowered preclinical studies, others could be due to a lack of understanding of disease processes occurring long before end-stage disease. Here we show the ability of a two-hit model that links genetic susceptibility with an environmental trigger (injury) to map sequential cellular changes that could underlie ALS disease pathogenesis. This model that coordinates the disease process at a precise time of onset could help develop therapeutics targeted at earlier stages of the disease and may translate better in clinical trials.

Conflict of interest

The authors declare no conflicts of interest.

Acknowledgements

This work was supported in part by the Patrick Grange Memorial Foundation.

References

Alexander, J.J., Anderson, A.J., Barnum, S.R., Stevens, B., Tenner, A.J., 2008. The complement cascade: Yin-Yang in neuro-inflammation neuro-protection and –degeneration. J. Neurochem. 107 (5), 1169–1187.
Anderson, E.N., Gochenaur, L., Singh, A., Grant, R., Patel, K., Watkins, S., Wu, J.Y., Pandey, U.B., 2018. Traumatic injury induces stress granule formation and enhances motor dysfunctions in ALS/FTD models. Human Mol. Gen. 27 (8), 1366–1381.
Blasco, H., Mavel, S., Corcia, P., Gordon, P.H., 2014. The glutamate hypothesis in ALS: pathophysiology and drug development. Curr. Mec. Chem. 1 (31), 3551–3575.
Calvo, M., Zhu, N., Tsantoulas, C., Ma, Z., Grist, J., Loeb, J.A., Bennett, D.L., 2010. Neuregulin-ErbB signaling promotes microglial proliferation and chemotaxis contributing to microgliosis and pain after peripheral nerve injury. J. Neurosci. 30 (15), 5437–5450.
Calvo, M., Dawes, J.M., Bennett, D.L., 2012. The role of the immune system in the generation of neuropathic pain. Lancet Neurol. 1 (7), 629–642.
Chen, H., Richard, M., Sandler, D.P., Umbach, D.M., Kamel, F., 2007. Head injury and amyotrophic lateral sclerosis. Am. J. Epidemiol. 166 (7), 810–816.
David, S., Greenhalgh, A.D., Kroner, A., 2015. Macrophage and microglial plasticity in the injured spinal cord. Neuroscience 307, 311–318.
Davis-Dusenbery, B.N., Williams, L.A., Klim, J.R., Eggan, K., 2014. How to make spinal motor neurons. Development 141 (3), 491–501.
Drachman, D.B., Chaudhry, V., Cornblath, D., Kuncl, R.W., Pestronk, A., Clawson, L., Mellits, E.D., Quaskey, S., Quinn, T., Calkins, A., 1994. Trial of immunosuppression in Amyotrophic Lateral Sclerosis using total lymphoid irradiation. Ann. Neurol. 5 (2), 142–150.
Esper, R.M., Loeb, J.A., 2004. Rapid axoglial signaling mediated by neuregulin and neurotrophic factors. J. Neurosci. 24 (27), 6218–6227.
Esper, R.M., Loeb, J.A., 2009. Neurotrophins induce neuregulin release through protein kinase Cdelta activation. J. Biol. Chem. 284 (39), 26251–26260.
Fournier, C.N., Schoenfeld, D., Berry, J.D., Cudkowicz, M.E., Chan, J., Quinn, C., Brown, R.H., Salameh, J.S., Tansey, M.G., Beers, D.R., Appel, S.H., Glass, J.D., 2018. An open label study of a novel immunosuppression intervention for the treatment of Amyotrophic Lateral Sclerosis. Amyotroph. Lateral Scler. Frontotemporal. Degener. 19 (3–4), 242–249.
Franz, C.K., Quach, E.T., Krudy, C.A., Federici, T., Kliem, M.A., 2009. A conditioning lesion provides selective protection in a rat model of Amyotrophic Lateral Sclerosis. PLoS One 4 (10), e7357.
Gordon, P.H., Moore, D.H., Miller, R.G., Florence, J.M., Verheijde, J.L., Doorish, C., Hilton, J.F., Spitalny, G.M., MacArthur, R.B., Mitsumoto, H., Neville, H.E., Boylan, K., Mozaffar, T., Belsh, J.M., Ravits, J., Bedlack, R.S., Graves, M.C., McCluskey, L.F., Barohn, R.J., Tandan, R., Western ALS Study Group, 2007. Efficacy of minocycline in patients with Amyotrophic Lateral Sclerosis: a phase III randomized trial. Lancet Neurol. 6 (12), 1045–1053.
Haley, R.W., 2003. Excess incidence of ALS in young Gulf War veterans. Neurology 61, 750–756.
Horner, R.D., Kamins, K.G., Feussner, J.R., Grambow, S.C., Hoff-Lindquist, J., Harati, Y., Mitsumoto, H., Pascuzzi, R., Spencer, P.S., Tim, R., Howard, D., Smith, T.C., Ryan, M.A.K., Coffman, C.J., Kasarskis, E.J., 2003. Occurrence of amyotrophic lateral sclerosis among Gulf War veterans. Neurology 61, 742–749.
Howland, D.S., Liu, J., She, Y., Goad, B., Maragakis, N.J., Kim, B., Erickson, J., Kulik, J., DeVito, L., Psaltis, G., DeGennaro, L.J., Cleveland, D.W., Rothstein, J.D., 2002. Focal loss of the glutamate transporter EAAT2 in a transgenic rat model of SOD1 mutant-mediated amyotrophic lateral sclerosis (ALS). PNAS 99 (3), 1604–1609.
Hulata, D., Hughes, W.F., Shott, S., Kroin, J.S., Gonzalez, M.H., Kerns, J.M., 2008. Early behavioral and histological outcomes following a novel traumatic partial nerve lesion. J. Neurosci. Meth. 172 (2), 236–244.
Kanning, K.C., Kaplan, A., Henderson, C.E., 2010. Motor neuron diversity in development and disease. Annu. Rev. Neurosci. 33, 409–440.
Kedersha, N., Ivanov, P., Anderson, P., 2013. Stress granules and cell signaling: more than just a passing phase? Trends Biochem. Sci. 38 (10).
Kerns, J.M., Braverman, B., Mathew, A., Lucchinetti, C., Ivankovich, A.D., 1991 Oct. A comparison of cryoprobe and crush lesions in the rat sciatic nerve. Pain 47 (1), 31–39.
Kerns, J.M., Hinsman, E.J., 1973. Neuroglial response to sciatic neurectomy. I. Light microscopy and autoradiography. J. Comp. Neurol. 151, 237–254.
Kigerl, K.A., Gensel, J.C., Ankeny, D.P., Alexander, J.K., Donnelly, D.J., Popovich, P.G., 2009. Identification of two distinct macrophage subsets with divergent effects causing either neurotoxicity or regeneration in the injured mouse spinal cord. J. Neurosci. 29 (43), 13435–13444.
Koka, R., Hadlock, T.A., 2001. Quantification of functional recovery following rat sciatic nerve transection. Exp. Neurol. 168 (1), 192–195.
Kong, J., Xu, Z., 1999. Peripheral axotomy slows motoneuron degeneration in a

transgenic mouse line expressing mutant SOD1 G93A. J. Comp. Neurol. 412, 373–380.
Lehman, E.J., Hein, M.J., Baron, S.L., Gersic, C.M., 2012. Neurodegenerative causes of death among retired National Football League players. Neurology 79 (19), 1970–1974.
Li, Y.R., King, O.D., Shorter, J., Gitler, A.D., 2013. Stress granules as crucibles of ALS pathogenesis. J. Cell Biol. 201 (3), 361–372.
Liddelow, S.A., Guttenplan, K.A., Clarke, L.E., Bennett, F.C., Bohlen, C.J., Schirmer, L., Bennett, M.L., Münch, A.E., Chung, W.S., Peterson, T.C., Wilton, D.K., Frouin, A., Napier, B.A., Panicker, N., Kumar, M., Buckwalter, M.S., Rowitch, D.H., Dawson, V.L., Dawson, T.M., Stevens, B., Barres, B.A., 2017. Neurotoxic reactive astrocytes are induced by activated microglia. Nature 541 (7638), 481–487.
Liu, J., Allender, E., Wang, J., Simpson, E.H., Loeb, J.A., Song, F., 2018. Slowing disease progression in the SOD1 mouse model by blocking neuregulin-induced microglial activation. Neurobiol. Dis. 111, 118–126.
Liu-Yesucevitz, L., Bilgutay, A., Zhang, Y.J., Vanderweyde, T., Citro, A., Mehta, T., Zaarur, N., McKee, A., Bowser, R., Sherman, M., Petrucelli, L., Wolozin, B., 2010. Tar DNA binding protein-43 (TDP-43) associates with stress granules: analysis of cultured cells and pathological brain tissue. PLoS One 5 (10), e13250 11.
Luo, C., Kuner, T., Kuner, R., 2014. Synaptic plasticity in pathological pain. Trends Neurosci. 37 (6), 343–355.
Calvo, M., Zhu, N., Tsantoulas, C., Ma, Z., Grist, J., Loeb, J.A., Bennett, D.L., 2011. Following nerve injury neuregulin-1 drives microglial proliferation and neuropathic pain via the MEK/ERK pathway. Glia 59 (4), 554–568.
Mariotti, R., Cristino, L., Bressan, C., Boscolo, S., Bentivoglio, M., 2002. Altered reaction of facial motoneurons to axonal damage in the presymptomatic phase of a murine model of familial amyotrophic lateral sclerosis. Neuroscience 115, 331–335.
Miranda, M.L., Alicia Overstreet Galeano, M., Tassone, E., Allen, K.D., Horner, R.D., 2008. Spatial analysis of the etiology of amyotrophic lateral sclerosis among 1991 Gulf War veterans. Neurotoxicology 29, 964–970.
Mitsumoto, H., Brooks, B.R., Silani, V., 2014. Clinical trials in Amyotrophic Lateral Sclerosis: why so many negative trials and how can trials be improved? Lancet Neurol. 13 (11), 1127–1138.
Moreno-Lopez, B., Sunico, C.R., Gonzalez-Forero, D., 2011. NO orchestrates the loss of synaptic boutons from adult “sick” motoneurons: modeling a molecular mechanism. Mol. Neurobiol. 43, 41–66.
Nagai, M., Re, D.B., Nagata, T., Chalazonitis, A., Jessell, T.M., Wichterle, H., Przedborski, S., 2007. Astrocytes expressing ALS-linked mutated SOD1 release factors selectively toxic to motor neurons. Nat. Neurosci. 10 (5), 615–622.
Philips, T., Rothstein, J.D., 2015. Rodent models of Amyotrohpic Lateral Sclerosis. Curr. Protoc. Pharmacol. 69, 5.67.1–5.67.21.
Piazza, O., Sirén, A.L., Ehrenreich, H., 2004. Soccer, neurotrauma and amyotrophic lateral sclerosis: is there a connection? Curr. Med. Res. Opin. 20 (4), 505–508.
Ravits, J.M., La Spada, A.R., 2009. ALS motor phenotype heterogeneity, focality, and spread. Neurology 73, 805–811.
Riggs, J.E., 1985. Trauma and amyotrophic lateral sclerosis. Arch. Neurol. 42, 205.
Riggs, J.E., 1993. Antecedent trauma and amyotrophic lateral sclerosis in young adult men. Mil. Med. 158, 55–57.
Riggs, J.E., 1995. Trauma, axonal injury, and amyotrophic lateral sclerosis: a clinical correlate of a neuropharmacologic model. Clin. Neuropharmacol. 18, 273–276.
Riggs, J.E., 2001. The latency between traumatic axonal injury and the onset of amyotrophic lateral sclerosis in young adult men. Mil. Med. 166, 731–732.
Sharp, P.S., Dick, J.R., Greensmith, L., 2005. The effect of peripheral nerve injury on disease progression in the SOD1(G93A) mouse model of amyotrophic lateral sclerosis. Neuroscience 130, 897–910.
Sharp, P.S., Tyreman, N., Jones, K.E., Gordon, T., 2018. Crush injury to motor nerves in the G93A transgenic mouse model of amyotrophic lateral sclerosis promotes muscle reinnervation and survival of functionally intact nerve-muscle contacts. Neurobiol. Dis. 113, 33–44.
Smittkamp, S.E., Spalding, H.N., Brown, J.W., Gupte, A.A., Chen, J., Nishimune, H., Geiger, P.C., Stanford, J.A., 2010. Measure of bulbar and spinal motor function, muscle innervation, and mitochondrial function of ALS rats. Behav. Brain Res. 211 (1), 48–57.
Song, F., Chiang, P., Wang, J., Ravits, J., Loeb, J.A., 2012. Aberrant neuregulin 1 signaling in Amyotrophic Lateral Sclerosis. J. Neuropathol. Exp. Neurol. 71 (2), 104–115.
Song, F., Chiang, P., Ravits, J., Loeb, J.A., 2014. Activation of microglial neuregulin1 signaling in the corticospinal tracts of ALS patients with upper motor neuron signs. Amyotroph. Lateral Scler. Frontotemporal. Degener. 15 (1–2), 77–83.
Swett, J.E., Hong, C.Z., Miller, P.G., 1991. All peroneal motoneurons of the rat survive crush injury but some fail to reinnervate their original targets. J. Comp. Neurol. 304 (2), 234–252.
Swinnen, B., Robberect, W., 2014. The phenotypic variability of amyotrophic lateral sclerosis. Nat. Rev. Neurol. 10 (11), 661–670.
Urushitani, M., Sik, A., Sakuai, T., Nukina, N., Takahashi, R., Julien, J.P., 2005. Chromogranin-mediated secretion of mutant superoxide dismutase proteins linked to amyotrophic lateral sclerosis. Nat. Neurosci. 9 (1), 108–118.
Valdes, E., Garbuzova-Davis, S., 2013. Brain and spinal cord trauma as a risk factor for amyotrophic lateral sclerosis: a mini-review. Open J. Neurosci. 3 (4).
Visser, A.E., Rooney, J.P.K., D'Ovidio, F., Westeneng, H.J., RCH, Vermeulen, Beghi, E., Chio, A., Logroscino, G., Hardiman, O., Veldink, J.H., van den Berg, L.H., Euro-MOTOR consortium, 2018. Multicenre, cross-cultural, population-based, case-control study of physical activity as risk factor for amyotrophic lateral sclerosis. J. Neurol. Neurosurg. Psychiatry. https://doi.org/10.1136/jnnp-2017-317724. Published Online First: 23 April 2018.
Yamanaka, K., Boillee, S., Roberts, E.A., Garcia, M.L., McAlonis-Downes, M., Mikse, O.R., Cleveland, D.W., Goldstein, L.S.B., 2008. Mutant SOD1 in cell types other then motor neurons and oligodendrocytes accelerates onset of disease in ALS mice. PNAS 105 (21), 7594–7599.
Yip, P.K., Malaspina, A., 2012. A. Spinal cord trauma and the molecular point of no return. Mol. Neurodegener. 7 (6).